

The tubulin-depolymerising agent combretastatin-4 induces ectopic aster assembly and mitotic catastrophe in lung cancer cells H460

Chiara Cenciarelli · Caterina Tanzarella · Ilio Vitale · Claudio Pisano · Pasqualina Crateri · Stefania Meschini · Giuseppe Arancia · Antonio Antocchia

Published online: 2 April 2008
© Springer Science+Business Media, LLC 2008

Abstract The relationship between microtubular dynamics, dismantling of pericentriolar components and induction of apoptosis was analysed after exposure of H460 non-small lung cancer cells to anti-mitotic drugs. The microtubule destabilising agent, combretastatin-A4 (CA-4) led to microtubular array disorganization, arrest in mitosis and abnormal metaphases, accompanied by the presence of numerous centrosome-independent “star-like” structures containing tubulin and aggregates of pericentrosomal matrix components like γ -tubulin, pericentrin and ninein, whereas the structural integrity of centrioles was not affected by treatment. On the contrary, in condition of prolonged exposure or high concentrations of CA-4 such aggregates never formed. Treatment with 7.5 nM CA-4, which produced a high frequency “star-like” aggregates, was accompanied by mitotic catastrophe commitment characterized by translocation of the proapoptotic Bim protein to mitochondria activation of caspases-3/9 and DNA fragmentation as a result of either prolonged metaphase arrest or attempt of cells to divide. Drug concentrations which fail to block cells at mitosis were also unable to activate apoptosis. A detailed time-course analysis of cell cycle arrest and apoptosis indicated that after CA-4 washout

the number of metaphases with “star-like” structures decreased as a function of time and arrested cells proceeded in anaphase. After 4 h, the multiple α - and γ -tubulin aggregates coalesced into two well-defined spindles in a bipolar mitotic spindle organization. Overall, our findings suggest that the maintenance of microtubular integrity plays a relevant role in stabilising the pericentriolar matrix, whose dismantling can be associated with apoptosis after exposure to microtubule depolymerising agents.

Keywords CA-4 · Centrosome · Ninein · Gamma-tubulin · Pericentrin · Mitotic catastrophe · Bim

Introduction

Microtubule-damaging agents (MDAs), including destabilizers such as combretastatin, vinblastine and vincristine, and stabilizers such as paclitaxel and epothilone B, are effective chemotherapeutic drugs against a variety of cancers [1]. Both MDA classes have been shown to operate by binding to tubulin at different binding sites and with different sensitivities [2, 3], nevertheless the dose-dependent series of morphological alterations of the mitotic spindle and of chromosomal disposition, are nearly identical. Hence, abnormal spindles have been classified in five different classes (I–V) based on increasing degrees of microtubular disorganization [4]. In particular, the presence of “star-like” structures in the shape of mono- or polyasters emanating some drug-resistant short microtubules and condensed chromatin arranged in a “ball-shape” characterize stage III. On the contrary, in stage IV and V, mitotic cells display full disassembly of the mitotic spindle with aggregates of condensed chromosomes.

C. Cenciarelli · C. Tanzarella · I. Vitale · A. Antocchia (✉)
Department of Biology, University “Roma Tre”,
V.le Marconi 446, 00146 Rome, Italy
e-mail: antocchia@uniroma3.it

C. Pisano
SIGMA-TAU Industrie Farmaceutiche Riunite S.p.A,
Via Pontina km 30,400, 00040 Pomezia, Italy

P. Crateri · S. Meschini · G. Arancia
Department of Technology and Health, Istituto Superiore
di Sanità, Viale Regina Elena 299, 00161 Rome, Italy

MDAs also promote several effects on the spindle poles or centrosomes, including abnormal centriole structure, centrosome fragmentation [5] and inappropriate centrosome duplication [6]. The centrosome acts as the principal microtubule organizing center (MTOC) in mammalian cells [7, 8], and morphologically is composed of a pair of centrioles surrounded by an osmiophilic matrix termed pericentriolar material (PCM). Centrin is considered a non-matrix protein and a recognized marker of centrosome in that it localizes to the distal lumen of individual centrioles and their interconnecting fibers [9, 10]. A large body of evidence strongly indicates that γ -tubulin, which together with tubulin complex proteins 2 and 3 (GCP2/3), constitutes the γ -tubulin ring complex (γ -TuRC) localized at the proximal end of centrioles [9, 11] that is critical for microtubule nucleation “in vivo” [12–14]; PCM proteins, such as kendrin (PCNT2), C-NAP1, centrosomin, pericentrin, ninein and p150Glued, play major roles as scaffold [15–19] and microtubule-anchoring components, docking the γ -TuRC to the centrosome [9, 19].

Recently, it has been shown that agents with different cellular targets such as DNA or cytoskeleton components may promote the formation of “star-like” mitosis as a result of relocalization of γ -tubulin [3, 20, 21]. In this respect, recent evidences point to the centrosome as an important player in the response to genotoxic stress, by showing that centrosome disruption leads to arrest of cell cycle progression [22, 23]. Overall data collected suggest the existence of a centrosome-damage checkpoint which mediates both G₁/S [23] and the G₂/M transition [22]. Though some reports have addressed the relationship between radiation- or arsenite-induced centrosome over-duplication and cell death [21, 22, 24], the role played by centrosome injury occurring as result of microtubule depolymerisation caused by anti-mitotic agents has not been investigated in depth.

In this respect, combretastatin-A4 (CA-4) and its derivatives have proven to induce cell death in various tumor and normal cell lineages through a caspase-dependent or caspase-independent mitotic catastrophe mechanism [25–27]. The latter, is a consequence of mitotic delay in which cells with condensed chromatin undergo apoptosis during M-phase, or escape mitotic block and produce aberrant distribution of chromosomes in daughter cells resulting in multinucleated cells [28–31].

Based on our previous publications showing CA-4-induced caspase-dependent mitotic catastrophe in H460 cells [26], here we analyze in more detail drug-induced precocious modifications in the centrosome and mitotic apparatus that may be involved in the cascade of events ending in cell death.

Materials and methods

Cell cultures and treatments

The human non-small-cell lung cancer (NSCLC) cell line H460 was maintained in RPMI or DMEM with 10% (v/v) foetal calf serum, 2 mm L-glutamine, 5,000 UI/ml penicillin and 5 mg/ml streptomycin (all from Gibco, Paisly, UK). Cells were grown in a 5% CO₂ atmosphere at 37°C. Forty-eight hours before treatment 200,000 cells were seeded in 35 mm Petri dishes (Falcon, Becton Dickinson, Franklin Lakes, NJ, USA) containing sterile glass coverslips, whereas for time-lapse experiments cells were seeded in appropriate μ Slide I chamber slides (Ibidi, Germany).

Combretastatin A-4 (CA-4) (Sigma–Aldrich, St. Louis, MO, USA) and staurosporine (Sigma–Aldrich, St. Louis, MO, USA), were freshly dissolved in DMSO (dimethyl sulfoxide) prior to each experiment at 100-fold concentration. Cells were treated for 8 h with drugs, whereas control cultures received 1% (v/v) DMSO. IC₅₀ values obtained in cytotoxicity assay over 24 h of treatment were 5 nM for CA-4.

Mitotic index

Cells were fixed in 3:1 (v/v) absolute methanol:acetic acid for 30 min and stained with 5% (v/v) GIEMSA. The mitotic index was calculated by scoring mitotic figures in a total of 1,000 cells per experimental point in repeated experiments.

Immunofluorescence microscopy

Cells were fixed in absolute methanol for 10 min and in acetone for 20 s at –20°C. After washing with PBS, cells were incubated for 1 h at 37°C with 1:50 mouse anti- α -tubulin antibody (Sigma–Aldrich, St. Louis, MO, USA), 1:10 mouse anti- α -acetylated tubulin antibody, non-diluted mouse anti- γ -tubulin antibody (Sigma–Aldrich, St. Louis, MO, USA), 1:250 rabbit anti-ninein antibody (Abcam, Cambridge, UK) or 1:500 rabbit anti-pericentrine antibody (Novus Biologicals, Littleton, CO) in 2% (w/v) BSA/PBS. As an alternative, cells were permeabilized in 0.1% (v/v) Triton-X-100 in PBS, and incubated for 1 h at 37°C with 1:1,000 anti-centrine rabbit antibody (kindly provided by Dr. Bornens) and 1:1 mouse anti- γ -tubulin antibody (Sigma–Aldrich, St. Louis, MO, USA) in 3% (w/v) BSA/PBS. After primary antibody incubation, slides were rinsed in 1% (w/v) BSA/PBS and incubated for 1 h at 37°C with 1:30 FITC-conjugated secondary anti-mouse antibody (Vector Laboratories, Burlingame, CA, USA) FITC-conjugated secondary anti-rabbit antibody (Molecular Probes,

Oregon, USA) or with 1:100 Texas Red-conjugated secondary anti-mouse antibody (Amersham Biosciences, UK) in 2% (w/v) BSA/PBS.

DNA was counterstained for 10 min with 0.2 µg/ml 4',6-diamidino-2-phenylindole (DAPI, Sigma–Aldrich, St. Louis, MO, USA) and slides mounted with an anti-fade solution (Vectashield; Vector Laboratories, CA, USA).

Slides were analyzed by means of an Axiophot fluorescent microscope (Zeiss, Germany) equipped with a charged cooled device (CCD) camera. Image re-elaborated with Adobe Photoshop 7.0 software (Adobe Systems Inc. Mountain View, CA, USA). Experiments were repeated at least three times.

Transmission electron microscopy and confocal microscopy analyses

Methanol-fixed cells were permeabilized in 0.01% (v/v) Tween in PBS, and incubated for 1 h at 37°C with 1:50 mouse anti- α -tubulin antibody (Sigma–Aldrich, St. Louis, MO, USA); 1:50 rabbit anti- α -tubulin antibody (Immunological sciences); 1:1 mouse anti- γ -tubulin antibody (Sigma–Aldrich, St. Louis, MO, USA); 1:1 CREST anti-kinetochore antibody (Sigma–Aldrich, St. Louis, MO, USA) in 0.1% Tween/PBS. Then slides were rinsed in 1% (w/v) BSA/PBS and incubated for 1 h at RT with 1:30–1:100 FITC or Texas Red-conjugated secondary antibodies. CLSM analysis was performed as previously described [26]. Briefly, the excitation wavelengths used were 488 and 543 nm; emission lines were collected after passage through a DD488/543 filter in a spectral window ranging from 515 to 700 nm. Signals from different fluorescent probes were taken in sequential scan mode, allowing elimination of channel crosstalk. Co-localization was detected in an overlay model. Images were processed by using LCS (Leica Microsystems, Germany) and Adobe Photoshop 7.0 software (Adobe Systems, Inc.).

For transmission electron microscopy assessment, treated and untreated cells, grown to near confluence, were fixed and stained as previously described [32]. Ultrathin sections were examined with a Philips 208S electron microscope.

Protein extraction, immunoprecipitation and immunoblotting

Mitochondrial cell lysates have been prepared by using the Mitochondria Isolation Kit (Pierce, USA) according to manufacturer's instructions. Western Blot analyses has been performed as previously described [32] loading 40 µg of mitochondrial proteins. Filters were then incubated with 1 µg/ml of specific antibodies recognizing Bim (Cell Signaling, MA, USA), α -tubulin (Santa Cruz Biotechnology,

CA, USA) and CoxIV (Abcam, Cambridge, UK). Primary antibodies were detected using secondary anti-mouse or anti-rabbit antibodies HRP conjugates (Amersham Biosciences, Buckinghamshire, England) and visualized using the enhanced chemiluminescence detection system (Amersham Biosciences, Buckinghamshire, England).

Apoptosis assays

Several assays to assess apoptosis were performed at both single cell level and on whole cellular population. Time-lapse experiments were performed by using the Magic Red® (Immunochemistry Technologies, MN, USA) substrate according to the producer's protocol. This substrate easily penetrates the cell membrane, entering in a non-fluorescent state. If caspases 3–7 are present in an activated form, the substrate is cleaved off yielding a red fluorescent product. Cells were maintained in a 5% CO₂ atmosphere at 37°C by means of a microscope cage incubator (Pecon, Germany). Live cell imaging were carried out with a Leica TCS SP5 confocal microscopy.

The fluorogenic assay for Caspases-3 and -9 were performed as described (Vitale et al. 2006) using Ac-Asp-Glu-Val-Asp-7-amino-4-methylcoumarin (Ac-DEVD-AMC) and Ac-Leu-Glu-His-Asp-7-amino-4-methylcoumarin (Ac-LEHD-AMC) as substrates (all from Alexis Biochemicals, San Diego, CA, USA). Cleavage of the substrates was assessed by using an LS-50B fluorescence spectrometer (Perkin-Elmer, Norwalk, CT, USA).

Apoptosis induction was also analyzed by means of the in situ Fluorescent-FragEL™ DNA fragmentation kit (Oncogene Research Products, San Diego, CA, USA) according to the manufacturer's instructions by using a Galaxy flow cytometer (Dako, Glostrup, Denmark). For each sample, 10,000 events were collected. All experiments were repeated twice.

Results

Interfering with spindle microtubule-dynamics arrests cells at metaphase stage with misaligned chromosomes

H460 cells were incubated for 8 h with the “tubulin-depolymerising agent” CA-4 in a dose-range of 1–100 nM. Treatments caused a dose-dependent block of the cell cycle in mitosis (Fig. 1a). Cells were arrested mainly at metaphase stage as evaluated by GEMSA staining (Fig. 1b), with mitotic index values of 35 and 47% and with an anelophase ratio close to 0 at concentrations ≥ 5 nM for combretastatin (Fig. 1a).

After low concentrations of Ca-4 a high degree of metaphases showed misaligned chromosomes (approximately

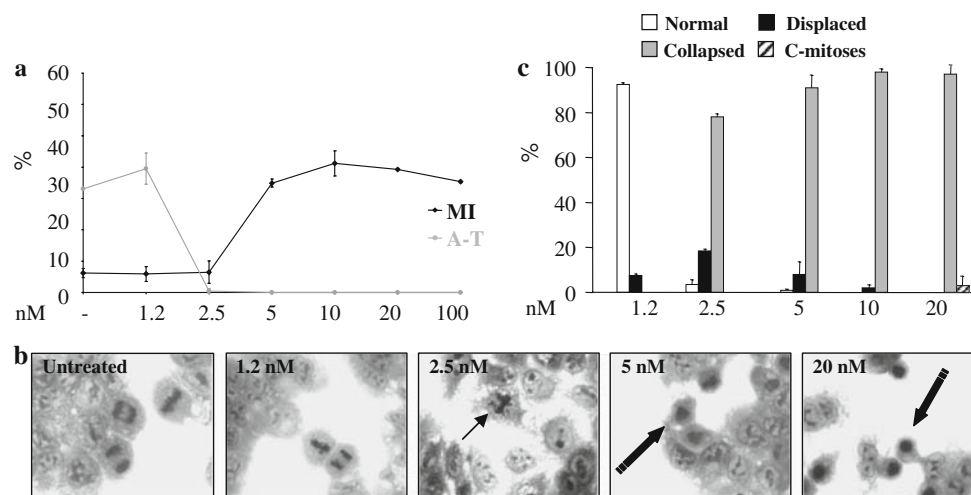


Fig. 1 CA-4 caused mitotic arrest and generation of abnormal metaphases in H460 cells (**a**, **b**). Mitotic index (MI) and anatelophase ratio (A-T) of H460 cells left untreated or treated for 8 h with different concentrations of CA-4 (**a**). Data are the mean of three independent experiments \pm SE. Metaphase organization in cells treated with CA-4 or (**c**). Mitoses were classified into four categories

based on the GIEMSA staining profiles: normal metaphases (normal), metaphases with displaced chromosomes (displaced, thin black arrow) or collapsed chromatin (thick black arrows), C-mitoses. Images are representative of three independent experiments. Panel c reports quantitative data recorded from three independent experiments (mean \pm SE)

20% at 2.5 nM) (Fig. 1c). With increasing concentrations the vast majority of combretastatin-treated cells presented collapsed chromatin (98% at 10 nM).

Combretastatin A-4 affects spindle organization giving rise to “star-like” mitosis

In both control and treated cells, the mitotic spindle arrangements were analyzed by immunostaining with antibodies directed against microtubules (α -, α -acetylated-tubulin) and centrosomes (γ -tubulin). Mitotic spindles of cells blocked in metaphase by low concentrations of combretastatin (0.1 nM) were bipolar with few chromosomes displaced from the metaphase plate and positioned in the vicinity of the spindle poles (spindle type stage I) (Fig. 2a). With increasing concentrations of combretastatin, spindle morphology became more abnormal and increasing numbers of chromosomes were located near the poles of a shorter bipolar spindle rather than in the metaphase plate (spindle type stage II) (not shown). After 7.5 nM CA-4 treatment many spindles (95%) had a multipolar organization with ball-shaped aggregations of condensed chromosomes containing multiple asters of microtubules (spindle types stage III and IV); this structure is called “star-like” (Fig. 2a). These small spindles contained residual kinetochore microtubules that were acetylated, as shown in immunostaining using an antibody that recognizes the acetylated form of α -tubulin (Fig. 2b). Acetylated microtubules are more stable and commonly resist to drug-induced disassembly [32].

The “star-like” structures were characterized by the presence of multiple signals of γ -tubulin (Fig. 2c), and occurred only in mitosis as observed after co-staining with phosphohistone H3 (not shown).

Following prolonged exposure or high concentrations of drug (≥ 20 nM) causing complete microtubules depolymerisation, non-centrosomal gamma-tubulin “star-like” structures did not form, whereas centrosomes retained γ -tubulin signals (spindle type stage V) (Fig. 2a–c).

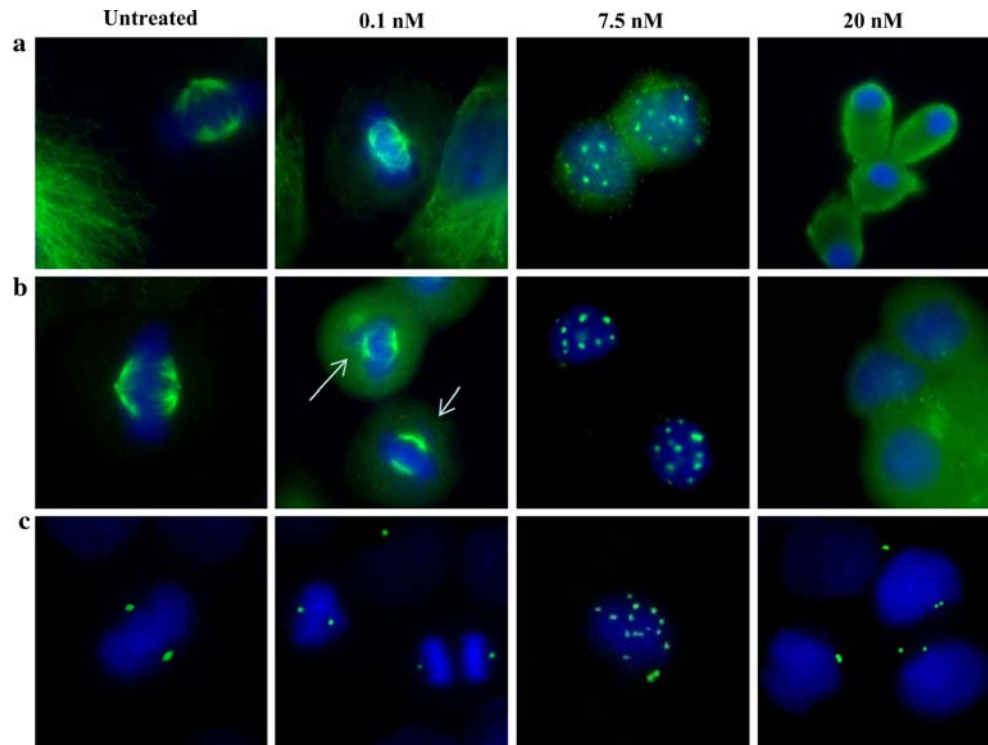
Immunoblot analysis aimed at quantitating the amount of γ -tubulin after combretastatin treatment showed no variation due to drug treatment (not shown).

Pericentriolar matrix components are present in CA-4-induced “star-like” structures

To better understand the spatial organization and the reciprocal localization of the components of the “star-like” structures, 7.5 nM combretastatin-treated cells were analyzed by transmission electron microscopy and by confocal microscopy, after immunolabeling with antibodies against α -tubulin, γ -tubulin, and CREST. After combretastatin treatment, γ -tubulin was located in close proximity to the chromosomes, at the center of a reduced monopolar spindle of α -tubulin that was connected to kinetochores and chromosomes (Fig. 3).

The localization of centrioles and of other centrosome or PCM components after CA-4 treatments was evaluated by fluorescence microscopy using specific antibodies against centrin, pericentrin, and ninein (Fig. 3c–e).

Fig. 2 Interferences in microtubular dynamics induce spindle abnormalities (a–c). Organization of mitotic spindles following treatment for 8 h with the indicated concentrations of CA-4 (a–c). Cells were stained with antibodies that specifically recognize α -tubulin (a), α -acetylated tubulin (b), or γ -tubulin (c) (all emitting in green). DNA was counterstained with DAPI. Representative examples of three independent experiments are shown. White arrows show chromosomes displaced from the metaphase plate. See the text for a detailed description of abnormal spindles



In control cells, two distinct dots of centrin that represent a pair of centrioles, co-localized with γ -tubulin, pericentrin, and ninein on each spindle pole (Fig. 3c–e).

On the other hand, in combretastatin-treated cells, the two dots of centrin co-localized only with one γ -tubulin pole of the multiple “star-like structures” (Fig. 3c); this means that the structural integrity of centrioles was not affected by treatment. In some cases four spots of centrine were visible in close proximity to each other, indicating that combretastatin also interfered with the centriole-pairs separation that occurred during early mitosis. Drug-induced “star-like” arrangements were also observed for pericentrin (Fig. 3d) and ninein (Fig. 3e).

Drug washout allows the reorganization of the combretastatin-induced dismantling of pericentriolar material and the establishment of normal bipolar mitotic spindles

Eight hours treatment followed by drug washout and recovery in fresh medium for different times showed that the number of “star-like” metaphases decreased as function of time (Fig. 4). After 4 h of post-treatment incubation, 97% of the drug-arrested metaphases could resume a normal pericentriolar matrix organization (two spots of γ -tubulin) and re-enter cell cycle with ana-telophase ratio value of 15.9%. Only a low percentage (4%) of anaphase was abnormal with lagging chromosomes (Fig. 4c). Time-lapse experiments after drug removal were

also performed to evaluate the fate of arrested cells which resumed cell cycle after drug removal (see below). About 75% of arrested cells resumed from the mitotic block were caspase-3 negative as evaluated after 12 h of drug wash out (Fig. 4f).

Combretastatin induces pericentriolar matrix dismantling and caspase-dependent mitotic catastrophe

To evaluate the relationship between redistribution of the pericentriolar matrix in the form of “star-like” structures and the apoptotic process, biochemical markers like mitochondrial translocation of BH3-only proteins, caspase activity and DNA fragmentation, were analyzed.

We performed experiments to determine the mitochondrial translocation of Bim. As shown, treatment with 7.5 nM CA-4 for 8 or 24 h determines a detectable enrichment of Bim in the mitochondrial protein fraction, suggesting a direct involvement of this protein in the MDA-induced apoptosis (Fig. 5a).

Caspase-involvement in CA-4-induced cell death was also analyzed at whole cellular level, in fluorogenic assays. In fact, a two- to threefold increase of caspase-9 and -3 expression was detected in cells exposed for 8 h to 7.5 nM CA-4. Such increase was even higher at 24 h with values ranging between three- and fourfold, and very close to values of caspase activation obtained after treatment with 2 μ M staurosporine for 6 h (Fig. 5b). After treatment with 7.5 nM CA-4 for 8 h, Caspase 3–7 activation was also

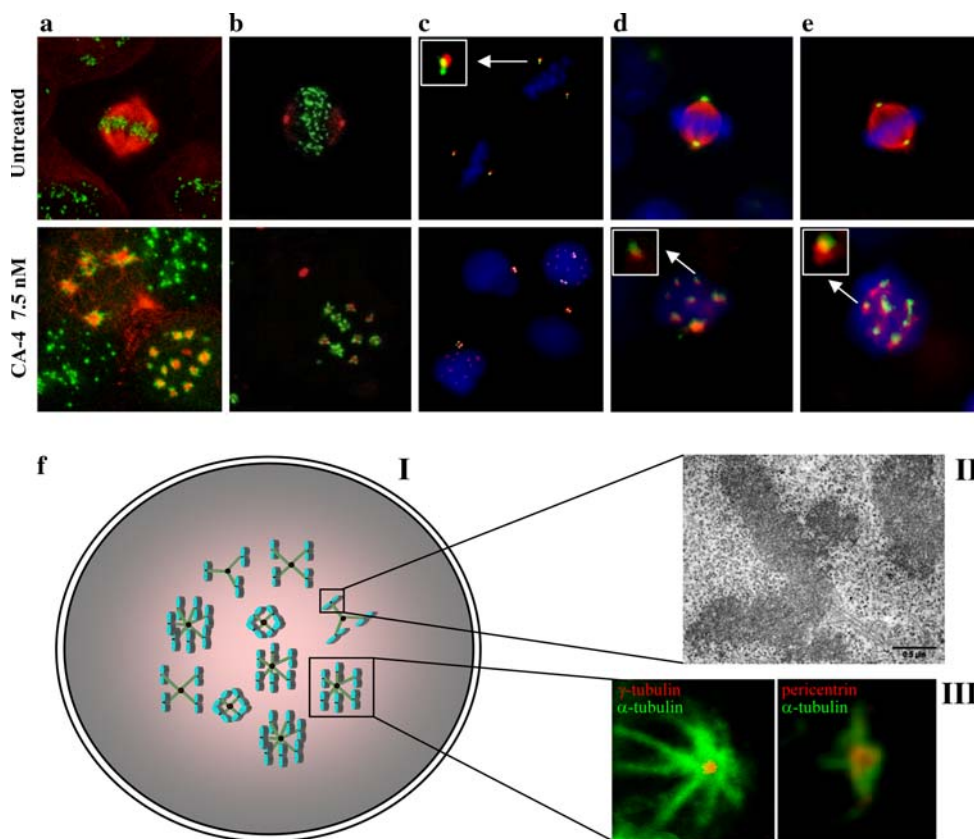


Fig. 3 Spatial arrangement of mitotic spindle and centrosome components upon CA-4 treatment. H460 cells were left untreated or treated for 8 h with 7.5 nM CA-4 prior to immunostaining with different combinations of antibodies and observation by fluorescence microscopy. The following co-immunostaining were performed: **(a)** CREST serum (green signal) and α -tubulin (in red). **(b)** CREST serum (in green) and γ -tubulin (in red). **(c)** γ -tubulin (in red) and centrin (in green) **(d)** α -tubulin (in red) and pericentrin (green). **(e)** α -tubulin (in red) and ninein (in green). In all cases DAPI was employed to counterstain DNA (in blue). Please note that the structural integrity of centrioles is not affected by the treatments (centrin, **c**), whereas the microtubular interference induced by CA-4 led to the generation of

the “star-like” structures accompanied by the dismantling of the PCM components (γ -tubulin, **b**; pericentrin, **d**; and ninein, **e**). **(f)** Proposed model of the arrangement of the “star-like” structure induced by CA-4 treatment (**I**). As observed by ultra structural assessment by TEM and by confocal microscopy co-immunostaining with antibodies specific for α -tubulin (in green) and γ -tubulin or pericentrin (red) (**II** and **III**, respectively), γ -tubulin and pericentrin are located at the center of each monopolar spindle, in turn composed of small and stable α -tubulin microtubules connected to kinetochores. Representative examples of three independent experiments are shown. See text for a detailed description

monitored at single cell level in time-lapse experiments by using the Magic Red substrate. Positive staining was observed in mitotic arrested cells as a result of a prolonged arrest which was not followed by resumption of cell cycle or attempt to divide, giving rise to a multinucleated cell (mitotic catastrophe) (Fig. 5c). Apoptosis was further confirmed by DNA fragmentation, evaluated by cytofluorimetric analysis after Fluorescent-FragELTM staining, showing about 40 and 90% apoptotic cells, at 8 and 24 h, respectively (Fig. 5d).

Discussion

By treating NSCLC H460 cells with CA-4, we found a dose-dependent mitotic arrest accompanied by an

increasing disorganization of chromosomal arrangement. In this respect, CA-4 behaved similarly to other drugs leading to chromosomal disposition according to stages I–V as described in cells treated with nocodazole or vinca-alkaloids [4]. Immunostaining of drug-induced stage III metaphases indicated the presence of multiple signals of α -tubulin and drug-disassembly resistant acetylated- α -tubulin [33], arranged in the shape of “star-like” structures. Such aggregates of α -tubulin could represent residual fragments of microtubules following the depolymerisation of mitotic spindle, ectopic centrosome-independent centres of microtubule nucleation, or splitting of pre-existing centrosomal material.

The γ -tubulin immunostaining allowed us to display differences in the effects obtained after treatment with either drug. The co-localization analysis carried out by

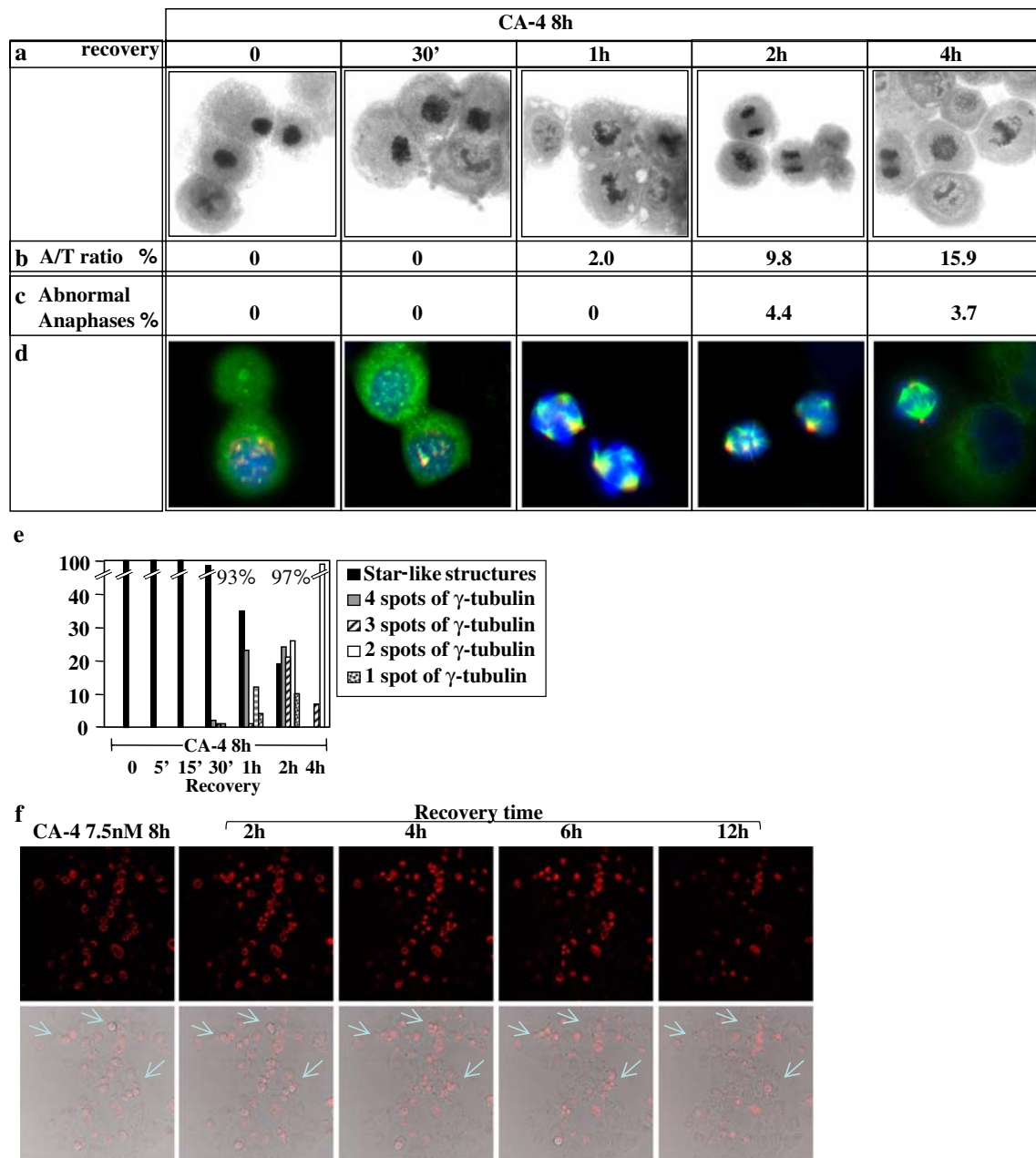


Fig. 4 Recovery in drug washout re-establishes structural and functional integrity of the mitotic spindle (**a, d**). H460 cells treated for 8 h with 7.5 nM CA-4 followed or not by recovery in drug-free conditions for the indicated time, were stained with GIEMSA (**a**) or co-immunostained with antibodies specific for α - or γ -tubulin (in green and red, respectively) (**b, c**). GIEMSA staining permitted the quantification of ana-telophase ratio (A-T) and of cells displaying abnormal anaphase, e.g., anaphase bridge or anaphase lagging (**a**). In

(**e**) the quantification of metaphase based on the number of γ -tubulin spots observed by fluorescence microscopy analysis is shown. Columns report the results of three independent experiments. Activation of caspases 3–7 have been analyzed after drug wash out using the magic red fluorescent substrate. Magic Red and BF images were collected at regular intervals throughout experiments; light blue arrows show arrested cells that resume from the mitotic block; selected images are shown in the panel (**f**)

confocal microscopy by using pairs of antibodies, together with TEM analysis and 3D image reconstruction, revealed that each “star-like” structure presents γ -tubulin at the centre of a spherical structure characterized by short drug-resistant microtubules connected to kinetochores. A “star-like” pattern of staining was also detected in stage III

metaphases obtained after treatment with colchicine, vinblastine, or combretastatin-derivatives [4, 26].

Though, agents like ionizing radiation [24, 34] or arsenic and its metabolites [22, 35, 36] have been shown to produce multiple centrosomal signals, the single detection of γ -tubulin for the centrosome did not allow us to

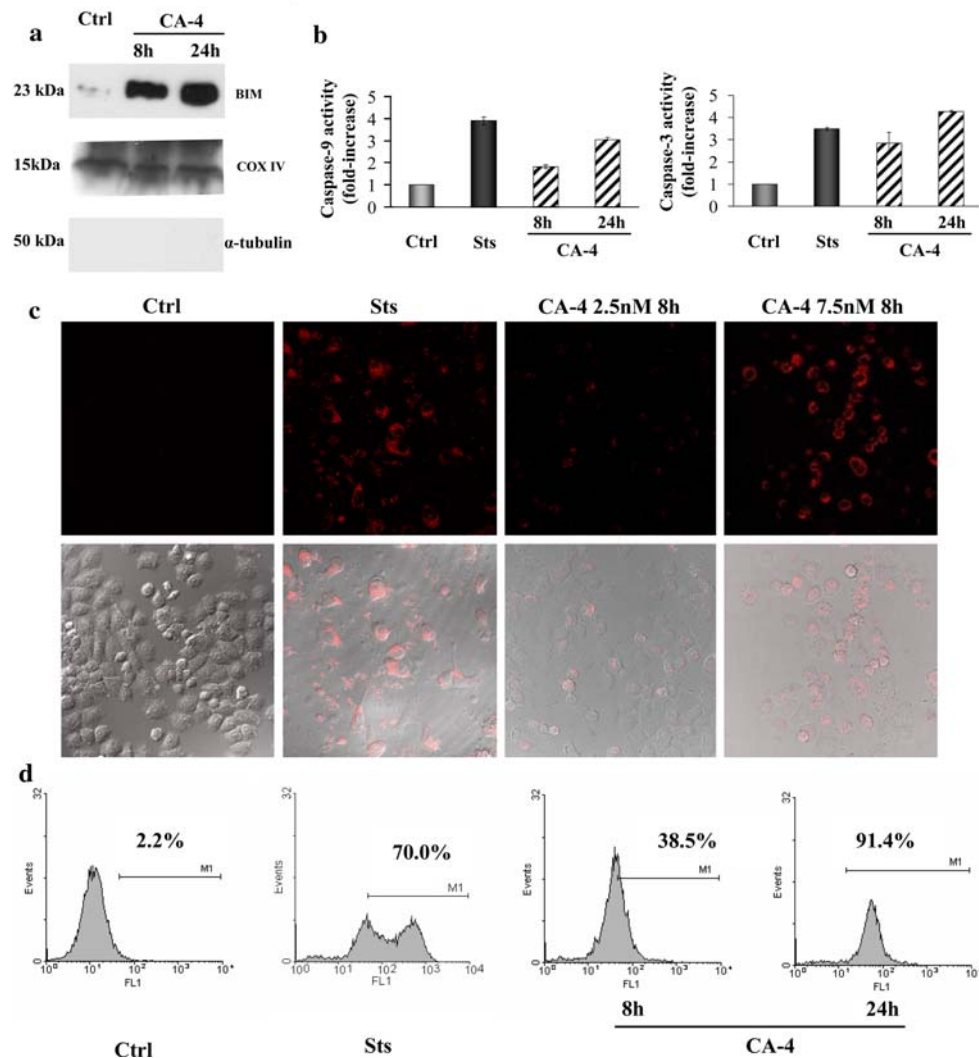


Fig. 5 PCM dismantling induced by CA-4 is followed by apoptosis induction. **(a)** Immunoblot analysis of mitochondrial fractions with the indicated antibodies. α -Tubulin and CoxIV were used as the cytosolic and mitochondrial protein marker, respectively. **(b)** Caspase-9 and -3 activities in protein extracts from cells left untreated or treated for 8 or 24 h with CA-4, as assessed by fluorogenic assays after incubation with caspase-9 (Ac-LEHD-AMC) or caspase-3 (Ac-DEVD-AMC) substrate. As a positive control, cells were treated for 4 h with 2 μ M staurosporine, a known activator of the caspases. Columns represent the fold increase in the activity of caspases as compared to untreated

cells. Results are expressed as the mean of three independent experiments \pm SE. **(b)** Activation of caspases 3–7 has been analyzed in untreated and treated cells using the magic red fluorescent substrate. Magic Red/BF or DIC images were collected at regular intervals throughout experiments; selected images are shown in the panel **(c)**. Cells were treated or not for the indicated time with CA-4, then analyzed for apoptosis-associated DNA fragmentation using Fluorescent-FragELTM DNA fragmentation kit by flow cytometry. The percentage of cells with cleaved DNA is reported. The results reported are representative of three independent experiments **(d)**

unambiguously distinguish between centrosome overduplication/fragmentation, dismantling of the centrosomal matrix or activation of ectopic assembly of nucleating centres. We found that in the majority of CA-4-treated cells the structural integrity of centrioles was not affected, as shown by the presence of two dots of centrine, a recognized marker of centrioles [9, 10], in both control and treated cells. In a few cells, however, four spots of centrine were visible in close proximity to each other, indicating that combretastatin might also affect centriole-pair separation,

which occurs during late in the G₂-phase, as observed in arsenite-treated cells [22]. Overall these findings led us to exclude true centriolar fragmentation or centrosome overduplication and favor a model based on disassembly and relocation of pericentriolar matrix after combretastatin treatment.

Moreover, we investigated the effect of microtubules perturbation on the release of centrosomal material which localizes either at the matrix, as the scaffold and anchoring protein pericentrin [9, 37], or to the subdistal appendages

of mother centriole, like the anchoring protein ninein [9, 38], which also promotes microtubules nucleation by docking the γ -TuRC at the centrosome [19]. Combretastatin was effective in displacing pericentrin as well as ninein from the centrosome, and in agreement with their role in γ -TuRC docking, cytoplasmic aggregates of pericentrin and ninein recruited γ -tubulin.

Cells displaying “star-like” structures recovered from mitotic block in drug-free conditions, though restart of microtubule nucleation began only after some hours, in spite of the presence of nucleating components. This may indicate the absence of additional centrosomal complexes required for activating the nucleation activity. Similarly, overexpression of ninein results in mislocalization of γ -tubulin, which is recruited to ectopic non-centrosomal ninein-containing sites which are, however, not active in nucleating microtubules [19, 39]. As a function of time in drug-free medium, probably through a mechanism of coalescence, the number of “star-like” structures decreased, then nucleation began and a normal bipolar mitotic spindle was established allowing cells to proceed from metaphase to anaphase. Though the transition from the “star-like” arrangement to the bipolar one was accompanied by the presence of monopolar and multipolar asters only a few lagging chromosomes were detected at anaphase, indicating that this transition can be overcome proficiently by cells once polymerisation has restarted. Furthermore, cells which resumed from the mitotic block were caspase-3 negative, indicating that the commitment to apoptosis occurs mainly as a response to a prolonged arrest or failure in cell division (see below).

Furthermore, our findings show that the “star-like” structures arise as a result of a critical level of drug-mediated microtubular disruption as evaluated in combined experiment with CA-4 and either a microtubule depolymerising agent (nocodazole) or a stabilising one (paclitaxel) (not shown). The observation that such structures occurred only at restricted concentrations or length of treatment, suggests that the maintenance of microtubule integrity in mitosis plays a relevant role in stabilising the interaction between pericentriolar matrix components and centrioles. In centrosome perturbed by centrosomin depletion [40], or in monastrol-treated cells it has been shown that kinetochores are able to enucleate microtubules [41], suggesting that γ -tubulin functions as a microtubule nucleator in the chromosome-mediated assembly pathway. Hence, the “star-like” structures might arise as result of the rescue of kinetochore microtubules that undergo drug-mediated catastrophe. As recently observed in yeast, plant and *Drosophila* cells [40, 42, 43], γ -tubulin can interact with pre-existing microtubules, so it is conceivable that, after partial depolymerisation, the centrosome-unassociated γ -tubulin cytoplasmic pool could bind to drug-resistant microtubules

at kinetochores. Then, through the presence of cytoplasmic complexes of γ -tubulin–pericentrin [44] or γ -tubulin–ninein interacting domains these proteins are concentrated to kinetochores giving rise to “star-like” structures. On the contrary, in the case of complete microtubule depolymerisation, as those occurring during mitosis at stage IV or by co-incubating cells with combretastatin and nocodazole, γ -tubulin would not have preformed microtubules to interact with, and therefore would be unable to recruit pericentrin and ninein complexes.

In this respect, recent studies have demonstrated that silencing of pericentrin A/B leads to uncoupling of the pericentrin– γ -TuRC interaction, disruption of astral microtubules and induction of apoptosis at the G₂/anaphase in U2OS cells [46]. In agreement with data obtained in HUVEC primary endothelial cells [25] we found that combretastatin-treated H460 cells accumulated in mitosis rather than in a G₂/anaphase stage, as shown by the level of chromosome condensation. These observations led us to rule out that combretastatin activates a G₂-phase checkpoint that senses spindle pole assembly/centrosome maturation because of disruption of the α -tubulin– γ -tubulin/pericentrin/ninein interaction. On the other hand, at these concentrations of drug, though the depolymerisation of α -tubulin is not complete, the mitotic spindle assembly checkpoint is activated as we previously showed in H460 cells [26]. We found that the appearance of mitosis with “star-like” structures occurred few hours after treatment with CA-4 and, at 8 h; they represented about 40% of the total cell population encompassing virtually all mitotic arrested cells.

The use of drug concentrations which failed to modify the mitotic index support the notion that the activation of the apoptotic process is strictly dependent on the mitotic block and level of tubulin polymerisation. It has been speculated that pro-apoptotic proteins sequestered by the microtubule network (such as the BH3-only protein Bim) might be released in response to microtubule depolymerisation, leading to caspase activation [44, 45]. Consistent with this hypothesis, we found Bim accumulation at level of mitochondria after CA-4-treatment and consequent caspase activation. In fact, in agreement with previous observations obtained in 24 h-treated cells [25, 26], the time-lapse analysis with a fluorescent substrate of caspase-3, as well as results gained by caspase activity assay and FragEL assays, indicates that after 8 h treatment, cells were committed to mitotic catastrophe mainly as a result of prolonged block. However, it should be noted that cell-type differences exist, in that contrastingly to the present and previous results on H460 cells [26], it was shown that CA-4 induced apoptosis through a caspase-dependent mechanism at least in human endothelial cells [25] and chronic lymphocytic leukemia cell lines [27].

Finally, the observation that in our experiments the frequency of “star-like” structures was not reduced by co-incubating combretastatin-treated cells with inhibitors of caspase-3, indicates that alterations in the tubulin network occurred upstream of caspase activation and not downstream (not shown). On the contrary, for other apoptotic agents, as UV light, anisomycin or TNF, it was shown that dismantling of the pericentriolar matrix from centrosome occurs as caspase-mediated event [46–48].

Conclusion

In conclusion, we show here that chemicals characterized by depolymerising activity like combretastatin A-4 release subclasses of proteins involved either in microtubule-nucleating or -scaffolding and -anchoring components of the centrosome, which organize in mitotic cells in the form of “star-like” structures. Combretastatin-treated H460 cells are killed via a mitotic catastrophe mechanism strictly dependent on the achievement of mitotic block, Bim translocation to mitochondria and caspase activation. The present results indicate that pericentriolar matrix dismantling does not occur as an effect of caspase-3 activation, rather it occurs upstream in response to the effect of tubulin-depolymerising agents.

Acknowledgments Chiara Cenciarelli is a PhD fellow at the Department of Biology, Università Roma Tre. This work was partly financed by SIGMA-TAU.

References

- Mollinedo F, Gajate C (2003) Microtubules, microtubule-interfering agents and apoptosis. *Apoptosis* 8:413–450
- Islam MN, Iskander MN (2004) Microtubulin binding sites as target for developing anticancer agents. *Mini Rev Med Chem* 4:1077–1104
- Jordan A, Hadfield JA, Lawrence NJ, McGown AT (1998) Tubulin as a target for anticancer drugs: agents which interact with the mitotic spindle. *Med Res Rev* 18:259–296
- Jordan MA, Thrower D, Wilson L (1992) Effects of vinblastine, podophyllotoxin and nocodazole on mitotic spindles. Implications for the role of microtubule dynamics in mitosis. *J Cell Sci* 102:401–416
- Wendell KL, Wilson L, Jordan MA (1993) Mitotic block in HeLa cells by vinblastine: ultrastructural changes in kinetochore-microtubule attachment and in centrosomes. *J Cell Sci* 104:261–274
- Fukasawa K, Choi T, Kuriyama R, Rulong S, Vande Woude GF (1996) Abnormal centrosome amplification in the absence of p53. *Science* 271:1744–1747
- Balczon R (1996) The centrosome in animal cells and its functional homologs in plant and yeast cells. *Int Rev Cytol* 169:25–82
- Doxsey S (2001) Re-evaluating centrosome function. *Nat Rev Mol Cell Biol* 2:688–698
- Bornens M (2002) Centrosome composition and microtubule anchoring mechanisms. *Curr Opin Cell Biol* 14:25–34
- Paoletti A, Moudjou M, Paintrand M, Salisbury JL, Bornens M (1996) Most of centrin in animal cells is not centrosome-associated and centrosomal centrin is confined to the distal lumen of centrioles. *J Cell Sci* 109:3089–3102
- Moudjou M, Bordes N, Paintrand M, Bornens M (1996) γ -Tubulin in mammalian cells: the centrosomal and the cytosolic forms. *J Cell Sci* 109:875–887
- Baas PW, Joshi HC (1992) Gamma-tubulin distribution in the neuron: implications for the origins of neuritic microtubules. *J Cell Biol* 119:171–178
- Joshi HC, Palacios MJ, McNamara L, Cleveland DW (1992) γ -tubulin is a centrosomal protein required for cell cycle-dependent microtubule nucleation. *Nature* 356:80–83
- Oakley CE, Oakley BR (1989) Identification of gamma-tubulin, a new member of the tubulin superfamily encoded by mipA gene of *Aspergillus nidulans*. *Nature* 338:662–664
- Quintyne NJ, Gill SR, Eckley DM, Crego CL, Compton DA, Schroer TA (1999) Dynactin is required for microtubule anchoring at centrosomes. *J Cell Biol* 147:321–334
- Askham JM, Vaughan KT, Goodson HV, Morrison EE (2002) Evidence that an interaction between EB1 and p150(Glued) is required for the formation and maintenance of a radial microtubule array anchored at the centrosome. *Mol Biol Cell* 13:3627–3645
- Quintyne NJ, Schroer TA (2002) Distinct cell cycle-dependent roles for dynactin and dynein at centrosomes. *J Cell Biol* 159:245–254
- Louie RK, Bahmanyar S, Siemers KA, Votin V, Chang P, Stearns T, Nelson WJ, Barth AI (2004) Adenomatous polyposis coli and EB1 localize in close proximity of the mother centriole and EB1 is a functional component of centrosomes. *J Cell Sci* 117:1117–1128
- Delgehr N, Sillibourne J, Bornens M (2005) Microtubule nucleation and anchoring at the centrosome are independent processes linked by ninein function. *J Cell Sci* 118:1565–1575
- Moisoi N, Erent M, Whyte S, Martin S, Bayley PM (2002) Calmodulin-containing substructures of the centrosomal matrix released by microtubule perturbation. *J Cell Sci* 115:2367–2379
- Dodson H, Wheatley SP, Morrison CG (2007) Involvement of centrosome amplification in radiation-induced mitotic catastrophe. *Cell Cycle* 6:364–370
- Yih LH, Tseng YY, Wu YC, Lee TC (2006) Induction of centrosome amplification during arsenite-induced mitotic arrest in CGL-2 cells. *Cancer Res* 66:2098–2106
- Mikule K, Delaval B, Kaldis P, Jurczyk A, Hergert P, Doxsey S (2007) Loss of centrosome integrity induces p38-p53-p21-dependent G₁-S arrest. *Nat Cell Biol* 9:160–170
- Sato N, Mizumoto K, Nakamura M, Ueno H, Minamishima YA, Farber JL, Tanaka M (2000) A possible role for centrosome overduplication in radiation-induced cell death. *Oncogene* 19:5281–5290
- Kanthou C, Greco O, Stratford A, Cook I, Knight R, Benzakour O, Tozer G (2004) The tubulin-binding agent combretastatin A-4-phosphate arrests endothelial cells in mitosis and induces mitotic cell death. *Am J Pathol* 165:1401–1411
- Vitale I, Antoccia A, Cenciarelli C, Crateri P, Meschini S, Arancia G, Pisano C, Tanzarella C (2007) Combretastatin CA-4 and combretastatin derivative induce mitotic catastrophe-dependent on spindle checkpoint and caspase-3 activation in non-small cell lung cancer cells. *Apoptosis* 12:155–166
- Nabha SM, Mohammad RM, Dandashi MH, Coupaye-Gerard B, Aboukameel A, Pettit GR, Al-Katib AM (2002) Combretastatin-A4 prodrug induces mitotic catastrophe in chronic lymphocytic

- leukemia cell line independent of caspase activation and poly(-ADP-ribose) polymerase cleavage. *Clin Cancer Res* 8:2735–2741
28. Castedo M, Perfettini JL, Roumier T, Yakushijin K, Horne D, Medema R, Kroemer G (2004) The cell cycle checkpoint kinase Chk2 is a negative regulator of mitotic catastrophe. *Oncogene* 23:4353–4361
 29. Castedo M, Perfettini JL, Roumier T, Andreau K, Medema R, Kroemer G (2004) Cell death by mitotic catastrophe: a molecular definition. *Oncogene* 23:2825–2837
 30. Roninson IB, Broude EV, Chang BD (2007) If not apoptosis then what? Treatment-induced senescence and mitotic catastrophe in tumor cells. *Drug Resist Updat* 4:303–313
 31. Ianzini F, Mackey MA (1997) Spontaneous premature chromosome condensation and mitotic catastrophe following irradiation of HeLa S3 cells. *Int J Radiat Biol* 72:409–421
 32. Vitale I, Antocchia A, Crateri P, Leone S, Arancia G, Tanzarella C (2005) Caspase-independent apoptosis is activated by diazepam-induced mitotic failure in HeLa cells, but not in human primary fibroblasts. *Apoptosis* 10:909–920
 33. Takemura R, Okabe S, Umeyama T, Kanai Y, Cowan NJ, Hirokawa N (1992) Increased microtubule stability and alpha tubulin acetylation in cells transfected with microtubule-associated protein MAP1B, MAP2 or tau. *J Cell Sci* 103:953–964
 34. Sato C, Kuriyama R, Nishizawa K (1983) Microtubule-organizing centers abnormal in number, structure, and nucleating activity in X-irradiated mammalian cells. *J Cell Biol* 96:776–782
 35. Ochi T, Nakajima F, Nasui M (1999) Distribution of gamma-tubulin in multipolar spindles and multinucleated cells induced by dimethylarsinic acid, a methylated derivative of inorganic arsenics, in Chinese hamster V79 cells. *Toxicology* 136:79–88
 36. Ochi T (2000) Induction of centrosome injury, multipolar spindles and multipolar division in cultured V79 cells exposed to dimethylarsinic acid: role for microtubules in centrosome dynamics. *Mutat Res* 454:21–33
 37. Dichtenberg JB, Zimmerman W, Sparks CA, Young A, Vidair C, Zheng Y, Carrington W, Fay FS, Doxsey SJ (1998) Pericentriolar and gamma-tubulin form a protein complex into a novel lattice at the centrosome. *J Cell Biol* 141:163–174
 38. Mogensen MM, Malik A, Piel M, Bouckson-Castaing V, Bornens M (2000) Microtubule minus-end anchorage at centrosomal and non-centrosomal sites: the role of ninein. *J Cell Sci* 113:3013–3023
 39. Stillwell EE, Zhou J, Joshi HC (2004) Human ninein is a centrosomal autoantigen recognized by CREST patient sera and plays a regulatory role in microtubule nucleation. *Cell Cycle* 3:923–930
 40. Mahoney M, Goshima G, Douglass AD, Vale RD (2006) Making microtubules and mitotic spindle in cells without functional centrosomes. *Curr Biol* 16:564–569
 41. Khodjakov A, Copenagle L, Gordon B, Compton DA, Kapoor TM (2003) Minus-end capture of preformed kinetochore fibers contribute to spindle morphogenesis. *J Cell Biol* 160:671–683
 42. Janson ME, Setty TG, Paoletti A, Tran PT (2005) Efficient formation of bipolar microtubule bundles requires microtubule-bound gamma-tubulin complexes. *J Cell Biol* 169:297–308
 43. Murata T, Sonobe S, Baskin TI, Hyodo S, Hasezawa S, Nagata T, Horio T, Hasebe M (2005) Microtubule-dependent microtubule nucleation based on recruitment of gamma-tubulin in higher plants. *Nat Cell Biol* 7:961–968
 44. Kroemer G, Galluzzi L, Brenner C (2007) Mitochondrial membrane permeabilization in cell death. *Physiol Rev* 87:99–163
 45. Yamaguchi H, Chen J, Bhalla K, Wang HG (2004) Regulation of bax activation and apoptotic response to microtubule-damaging agents by p53 transcription-dependent and -independent pathways. *J Biol Chem* 279:39431–39437
 46. Zimmerman WC, Sillibourne J, Rosa J, Doxsey SJ (2004) Mitosis-specific anchoring of gamma-tubulin complexes by pericentriolar controls spindle organization and mitotic entry. *Mol Biol Cell* 15:3642–3657
 47. Moss DK, Betin VM, Malesinski SD, Lane JD (2006) A novel role for microtubules in apoptotic chromatin dynamics and cellular fragmentation. *J Cell Sci* 119:2362–2374
 48. Moss DK, Lane JD (2006) Microtubules: forgotten players in the apoptotic execution phase. *Trends Cell Biol* 16:330–338